Insula serotonin 2A receptor binding and gene expression contribute to serotonin transporter polymorphism anxious phenotype in primates

Andrea M. Santangelo[a,b,1], Steve J. Sawiak[a,b,c], Tim Fryer[c], Young Hong[c], Yoshiro Shiba[a], Hannah F. Clarke[a,b], Patrick J. Riss[c], Valentina Ferrari[c], Roger Tait[b], John Suckling[c], Franklin I. Aigbirhio[c], and Angela C. Roberts[a,b]

[a]Department of Physiology, Development and Neuroscience, University of Cambridge, CB2 3DY Cambridge, United Kingdom; [b]Behavioural and Clinical Neuroscience Institute, University of Cambridge, CB2 3EB Cambridge, United Kingdom; and [c]Department of Clinical Neuroscience, Wolfson Brain Imaging Centre, University of Cambridge, CB2 0QQ, United Kingdom

Genetic variation in the serotonin transporter gene (*SLC6A4*) is associated with vulnerability to affective disorders and pharmacotherapy efficacy. We recently identified sequence polymorphisms in the common marmoset *SLC6A4* repeat region (AC/C/G and CT/T/C) associated with individual differences in anxiety-like trait, gene expression, and response to antidepressants. The mechanisms underlying the effects of these polymorphisms are unknown, but a key mediator of serotonin action is the serotonin 2A receptor ($5HT_{2A}$). Thus, we correlated $5HT_{2A}$ binding potential (BP) and RNA gene expression in 16 *SLC6A4* genotyped marmosets with responsivity to $5HT_{2A}$ antagonism during the human intruder test of anxiety. Voxel-based analysis and RNA measurements showed a reduction in $5HT_{2A}$ BP and gene expression specifically in the right posterior insula of individuals homozygous for the anxiety-related variant AC/C/G. These same marmosets displayed an anxiogenic, dose-dependent response to the human intruder after $5HT_{2A}$ pharmacological antagonism, while CT/T/C individuals showed no effect. A voxel-based correlation analysis, independent of *SLC6A4* genotype, revealed that $5HT_{2A}$ BP in the adjacent right anterior insula and insula proisocortex was negatively correlated with trait anxiety scores. Moreover, $5HT_{2A}$ BP in both regions was a good predictor of the size and direction of the acute emotional response to the human intruder threat after $5HT_{2A}$ antagonism. Our findings suggest that genetic variation in the *SLC6A4* repeat region may contribute to the trait anxious phenotype via neurochemical changes in brain areas implicated in interoceptive and emotional processing, with a critical role for the right insula $5HT_{2A}$ in the regulation of affective responses to threat.

serotonin transporter polymorphism | insula cortex | serotonin 2A receptor | anxiety

G enetic variation in the serotonin transporter gene (*SLC6A4*) has been associated with early life stress reactivity, vulnerability to affective disorders, and altered social cognition (1). Specifically, a variable number of tandem repeats (VNTR) located upstream of the promoter region have been identified in human and non-human primates, with short alleles being linked to reduced gene expression and emotionally vulnerable phenotypes (2, 3). Neuroimaging studies have provided strong evidence supporting these gene-behavioral associations and suggest neurodevelopmental mechanisms underlying the *SLC6A4* genetic variation. Individuals carrying the short alleles show hyperactivity to threat-related stimuli (e.g., fearful faces or Pavlovian conditioned stimuli in humans, and a human intruder in macaques) or during negative self-reflection in a network of structures that consistently include the amygdala, insula, and dorsomedial pre-frontal/anterior cingulate cortex (4–11). Altered connectivity has also been reported between structures in this network and related areas, including medial, lateral, and orbital prefrontal cortex in short allele carriers (8, 12–14), suggesting impaired regulation of the emotional response. In particular, the right anterior insula has

been implicated in altered emotion regulation in short allele carriers (9, 15, 16). This key region integrates the interoceptive information from the posterior insula with cognitive processing from prefrontal areas, and it is hypothesized to form the subjective feeling of emotion and self-awareness, specifically with respect to negative affect (17, 18). In addition to these functional changes, reduced gray matter volume in areas involved in emotional processing, including the amygdala, medial prefrontal cortex, and hippocampus, have also been described in short allele carriers (12, 19). Finally, although serotonin transporter binding studies have not provided consistent results (19–22), reduced serotonin 1A receptor binding in cortical areas has been reported in short allele carriers, both in humans and macaques (23, 24).

Polymorphisms in *SLC6A4* have also been associated with treatment efficacy of selective serotonin reuptake inhibitors (SSRIs), with short allele carriers showing a slower remission rate and more severe side effects (25). While SSRIs are the most widely used drugs for the treatment of anxiety and depression, 1/3 of the patients show a poor response (26), and it has been proposed that the anxiety experienced by some patients at the early stages of

---

Significance

Serotonin transporter polymorphisms within the primate-specific promoter repeat region are associated with altered emotion regulation, vulnerability to psychiatric disorders, and differences in antidepressant responsiveness. However, the underlying neurobiological mechanisms are poorly understood. Using positron emission tomography imaging, a behavioral anxiety test, and post-mortem expression measurements, we show that marmoset monkeys carrying a high anxiety-related serotonin transporter variant have reduced serotonin 2A receptor ($5HT_{2A}$) binding and RNA expression in right posterior insula and differential sensitivity to anxiogenic effects of acute $5HT_{2A}$ antagonism, the latter predicted by $5HT_{2A}$ binding in adjacent right anterior insula and insula proisocortex. Our findings highlight the value of marmosets in studying gene–brain–behavior relationships and may contribute to genetic and imaging screens development in personalized medicine for treating anxiety.

treatment may contribute to this reduced treatment efficacy (27). In some SSRI-resistant patients, a therapy combining SSRIs with serotonin 2 receptor ($5HT_2$) antagonists has been shown to improve the efficacy of the antidepressant treatment (27–29). However, the mechanisms by which $5HT_2$ regulates the emotional response are still unknown and vary according to the specific brain areas and the type of behaviors measured (28). Reports studying brain serotonin receptor alterations have provided conflicting results with respect to depression (30), and little is known about anxiety disorders. However, the density of medial prefrontal cortex serotonin 2A receptor ($5HT_{2A}$) does correlate negatively with right amygdala reactivity to threat stimuli (fearful faces) (31), but only when $5HT_{1A}$ binding is relatively low (32). In addition, a positron emission tomography (PET) imaging study in monozygotic twins suggests that ~40 to 50% of interindividual variability in cortical $5HT_{2A}$ density is genetically driven (33). However, whether the *SLC6A4* polymorphisms contribute to alterations in cortical $5HT_{2A}$ density, and subsequently to the anxious phenotype, has not yet been explored.

Studies in animals can provide a detailed mechanistic understanding of the brain–behavior interactions related to this polymorphism, but other than humans, the *SLC6A4* repeat region has only been found in primates, including apes and monkeys, but not in prosimians or rodents (2). Moreover, a VNTR within the *SLC6A4* repeat region has only been reported in humans and Old World monkeys, but not in New World monkeys such as marmosets (34). However, we recently identified sequence variation within the common marmoset *SLC6A4* repeat region that revealed a difference in *SLC6A4* RNA expression patterns and sensitivity to threat stimuli similar to that of the human and macaque *SLC6A4* VNTR. Thus, marmosets carrying the low-expressing haplotype (AC/C/G) show an enhanced anxiety-like behavioral repertoire toward a human intruder threat compared with marmosets carrying the high-expressing variant (CT/T/C) (35). Moreover, these 2 haplotypes are associated with, respectively, opposing anxiogenic and anxiolytic effects of acute administration of the SSRI citalopram during the human intruder threat, effects that were specifically associated with the average distance maintained from, and reflecting avoidance of, the human intruder, without changing the overall behavioral repertoire. Such genotype-dependent differential sensitivity to the acute effects of an SSRI may underlie, at least in part, differential sensitivity to pharmacotherapy in people with anxiety and depression (35).

The marmoset's small size, short gestation period, and accelerated development compared with Old World monkeys, alongside its sophisticated social and emotional behavior (36, 37) and primate brain with expanded associated neocortex compared with rodents, make it an ideal species for laboratory studies of gene–brain–behavior interactions during development and adulthood (38). Moreover, the use of marmosets that are bred "in house" affords considerable control/restriction over the environmental influences during development, thereby helping to expose the influence of genetic variation. Thus, taking advantage of this newly discovered polymorphism in marmosets, the relationship between cortical $5-HT_{2A}$ density and the anxious phenotype in the 2 *SLC6A4* homozygous haplotypes was determined. We employed a unique combination of PET imaging of the $5HT_{2A}$-specific radioligand [^{18}F]altanserin (39) and psychopharmacological challenge with a $5-HT_{2A}$ antagonist in vivo, followed by measurements of post-mortem $5-HT_{2A}$ RNA expression in those brain regions showing differential altanserin binding. Based on the neurobiological changes reported in short allele carriers mentioned above, and the relationship between cortical $5-HT_{2A}$ density and amygdala reactivity, we hypothesized that marmosets homozygous for the AC/C/G anxiety-related haplotype may show reduced $5-HT_{2A}$ binding in brain areas implicated in emotional processing compared with the low anxious CT/T/C homozygous.

To define the relationship between genotype, brain $5-HT_{2A}$ receptors, and sensitivity to the behavioral effects of a $5HT_{2A}$ pharmacological challenge, we measured each marmoset's anxiety response to an unknown human (uncertain threat) after an acute dose of a specific $5-HT_{2A}$ antagonist (M100907) and investigated whether the response was related to $5-HT_{2A}$ binding potential (BP).

Results

Selective Reductions in $5HT_{2A}$ BP and Post-mortem RNA Levels in the Right Posterior Insula of Marmosets Homozygous for the High Anxiety-Related *SLC6A4* Haplotype AC/C/G. PET imaging of the $5HT_{2A}$-specific radioligand [^{18}F]altanserin (39) in a cohort of 16 marmosets, balanced by *SLC6A4* genotype and sex, revealed that whole-brain $5HT_{2A}$ BP did not differ significantly between genotypes (global signal AC/C/G vs. CT/T/C; 95% CI: −0.06 to 0.15; 2-tailed t test, $P = 0.36$). However, a voxel-based analysis identified one specific cluster within the right posterior insula (Fig. 1*A* and Table 1) that showed a 27.3% (95% CI [21, 34]) reduction of $5HT_{2A}$ BP in those animals carrying the anxiety-related AC/C/G haplotype compared with those carrying the CT/T/C haplotype (one-way ANOVA: $F_{(1,15)} = 78.72$, $P = 4.02E-07$; Fig. 1*B*). Consequently, a real-time PCR assay was performed on the right posterior insula post mortem, and this revealed paralleled findings. The expression of $5HT_{2A}$ RNA not only correlated positively with $5HT_{2A}$ BP (Pearson correlation: $r = 0.722$, $P = 0.005$; *SI Appendix*, Fig. S1*A*) but also showed a similar reduction in the animals homozygous for the anxiety-related AC/C/G haplotype (20.1%, 95% CI [10.4, 29.9]; one-way
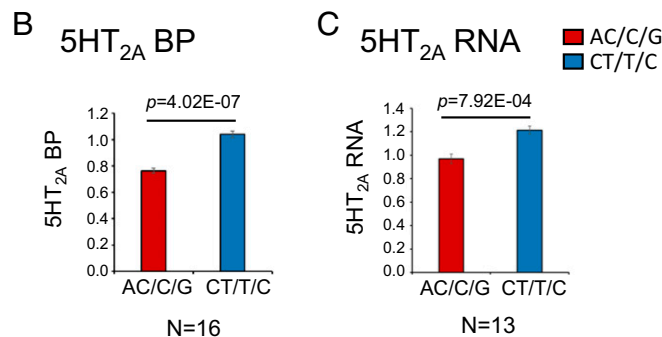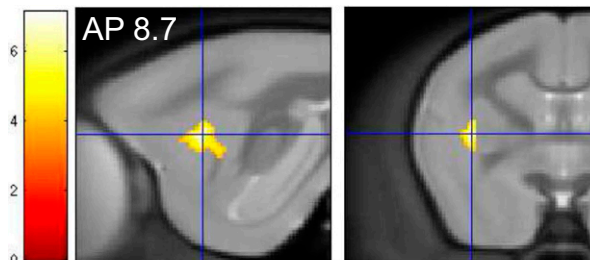
A Right posterior insula

B $5HT_{2A}$ BP   C $5HT_{2A}$ RNA

Fig. 1. Relation of $5HT_{2A}$ to *SLC6A4* variants. Voxel-based analysis of $5HT_{2A}$ BP comparing marmosets homozygous for the *SLC6A4* variants AC/C/G vs. CT/T/C. (*A*) Specific cluster in right posterior insula, with an anteroposterior (AP) coordinate of 8.7, in sagittal (*Left*) and coronal (*Right*) sections centered at the highest significant peak ($t = 7.14$). (*B*) Mean ± SEM $5HT_{2A}$ BP in the right posterior insula cluster for each homozygous group (AC/C/G < CT/T/C; one-way ANOVA: $F_{(1,15)} = 78.72$, $P = 4.02E-07$). (*C*) Mean ± SEM $5HT_{2A}$ RNA expression in the right posterior insula region obtained post mortem for each homozygous group (AC/C/G < CT/T/C; one-way ANOVA: $F_{(1,12)} = 20.96$, $P = 7.9E-04$). AP coordinates from ref. 70.

Table 1. Significant clusters derived from the voxel-based analysis of 5-HT$_{2A}$ BP

	Cluster extent, voxels	Cluster P	Peak level, t	Peak voxel left/right, mm*	Peak voxel ant/post, mm*	Peak voxel dors/vent, mm*	Structure name*
Contrast analysis between 5-HT$_{2A}$ BP of marmosets homozygous for the SLC6A4 genotypes, correction for multiple comparisons: $P < 0.05$ (FWE)							
Cluster 1	377	0.014[†]	7.14	−7.1	8.7	10.2	Posterior insula (DI, GI)
Correlational analysis between anxiety scores in the HI test (PC1) and 5-HT$_{2A}$ BP, correction for multiple comparisons: $P < 0.05$ (FWE)							
Cluster 1	88	0.001[‡]	4.01	−7.1	12.2	7.9	Anterior insula (Gu)
Cluster 2	57	0.001[‡]	3.73	−8.9	8.1	9.1	Insula proisocortex (IPro)

ant, anterior; DI, dysgranular insular cortex; dors, dorsal; GI, granular insular cortex; Gu, gustatory cortex; IPro, insular proisocortex; pos, posterior; vent, ventral.
*From ref. 70.
[†]Family-wise error (FWE)-corrected.
[‡]Uncorrected.

ANOVA: $F_{(1,12)} = 20.96$, $P = 7.9E-04$; Fig. 1C). To confirm the laterality of this effect, the right posterior insula cluster identified with PET was reflected about the midline to extract homologous values of 5-HT$_{2A}$ BP from the left hemisphere. While the left posterior insula similarly showed a significant reduction in 5HT$_{2A}$ BP in the AC/C/G group (one-way ANOVA: $F_{(1,15)} = 4.69$, $P = 0.048$; *SI Appendix*, Fig. S2G), it did not survive corrections for multiple comparisons. Likewise, RNA expression in the left posterior insula, which correlated positively with 5HT$_{2A}$ BP (Pearson correlation: $r = 0.633$, $P = 0.020$; *SI Appendix*, Fig. S1D), only showed a trend toward a reduction in the AC/C/G group (one-way ANOVA: $F_{(1,12)} = 4.26$, $P = 0.063$; *SI Appendix*, Fig. S3G).

SLC6A4 Genotype-Dependent Anxiogenic Response to Threat after Acute 5HT$_{2A}$ Antagonism in Marmosets Homozygous for the Anxiety-Related Haplotype AC/C/G. A previous study from our group has shown that the *SLC6A4* polymorphisms in marmosets are associated with anxiety-like trait, as measured by the human intruder test (HI test) (35). The HI test measures an array of behavioral responses directed toward an unfamiliar person staring at the marmoset for 2 min while the animal is in its home cage (Fig. 2A). The uncertain nature of this stimulus induces a pattern of anxiety-like behavior. A principal component analysis (PCA) of the array of behavioral variables, including vocalizations, locomotion, head bobbing, and distance from the intruder, revealed 2 principal components, PC1 (anxiety) and PC2 (coping strategy), which together explained the variability observed within the behavioral repertoire. Specifically, the AC/C/G homozygous marmosets presented increased trait anxiety (high PC1 scores) characterized by larger average distance from the human intruder, reduced locomotion and jumps to the front, and high numbers of head bobbing and Egg and Tse-like vigilant calls. In addition, they showed a passive coping strategy (low PC2 scores) driven mainly by low numbers of Tsik and Tsik-Egg aggression-related calls. Remarkably, the CT/T/C group showed the opposite pattern (35). Comparable to this large cohort ($n = 52$) from which the PCA was derived, the cohort in our current study ($n = 16$) showed a similar differential pattern for PC1 and PC2. However, as expected for polymorphisms presenting high frequency and low penetrance, such as those in the *SLC6A4* repeat region, the effects of genetic variation on phenotype in a small sample ($n = 16$ vs. $n = 52$) became weaker due to increased variation and reduced power, with only PC2 reaching statistical significance (a priori hypothesis: for PC1, AC/C/G > CT/T/C and for PC2, AC/C/G < CT/T/C; 1-tailed t test: PC1, $P = 0.07$ and PC2, $P = 0.03$; *SI Appendix*, Fig. S4 and Table S1).

Given that the present study revealed specific reductions in 5-HT$_{2A}$ in the right posterior insula of the anxiety-related AC/C/G group, we hypothesized that the anxiety-like response of the animals homozygous for this haplotype would be more

sensitive to 5-HT$_{2A}$ antagonism. To test this hypothesis, we administered a 5-HT$_{2A}$ antagonist (M100907) peripherally and measured the responsivity of marmosets to a human intruder using a repeated-measure block design (*Materials and Methods*).

Previous studies have shown that acute administration of anxiolytics (40) has a marked impact on average distance from the human threat (avoidance response), and we recently identified a *SLC6A4* genotype-dependent response to acute administration of the SSRI citalopram on this measure too, without altering the overall anxiety-like trait (i.e., PC1, PC2) (35). Thus, we focused the subsequent analysis of the acute effects of M100907 on average distance (*Materials and Methods*), although all other behavioral measures and PCA scores calculated for this pharmacological study are summarized in *SI Appendix*, Table S2. As predicted, after acute 5-HT$_{2A}$ pharmacological antagonism with the higher of the 2 doses administered, marmosets homozygous for the anxiety-related haplotype AC/C/G displayed an enhanced anxiogenic response to the human intruder, with a significant increase in average distance from the human intruder compared with vehicle (planned comparisons: vehicle vs. M100907: 0.3-mg/kg dose; paired 2-tailed t test: $P = 0.038$; Fig. 2B).
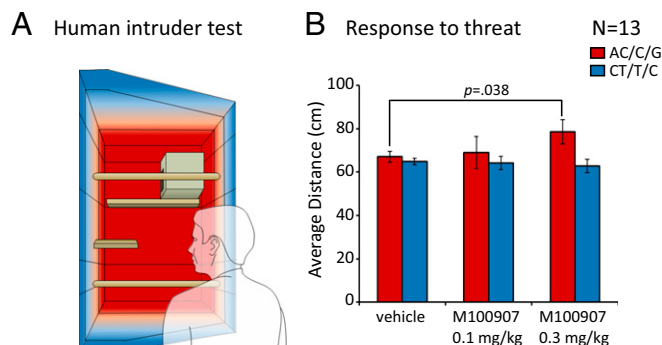

Fig. 2. *SLC6A4* genotype-dependent differential sensitivity to a 5HT$_{2A}$ antagonist during the HI test. (*A*) Schematic of the right top quadrant of the home cage, where the HI test takes place. An unfamiliar human stands in front of the cage and stares at the marmoset in the eyes for 2 min. Video and audio tapes were recorded, and behaviors were scored post hoc. Regions closer to the human intruder (corresponding to a less anxious-like state) are shown in blue, and regions further away from the human intruder (corresponding to a more anxious-like state) are shown in red. (*B*) Response to the human intruder threat after treatment with either vehicle or 5HT$_{2A}$-specific antagonist M100907 (low [0.1 mg/kg] and high [0.3 mg/kg] doses). Mean ± SEM of average distance from the unfamiliar human is presented for each group in each condition (AC/C/G: vehicle vs. high dose, planned comparison paired 2-tailed t test: $P = 0.038$).

NEUROSCIENCE

There was no effect of either dose in the CT/T/C group and no effects on any other measure (*SI Appendix*, Table S2).

Together, these results suggest a functional role for the observed genotype differences in $5HT_{2A}$ BP and RNA expression in the posterior insula in the regulation of anxiety-like behavior that may underlie their differences in trait anxiety.

$5-HT_{2A}$ BP and RNA Levels in the Right Anterior Insula and Insula Proisocortex Predict Trait Anxiety. To establish whether $5HT_{2A}$ BP in the posterior insula or anywhere else in the brain was related to trait anxiety per se, we performed a voxel-based analysis correlating $5-HT_{2A}$ BP with trait anxiety (PC1) and coping strategy (PC2) scores of the present cohort of marmosets, independent of *SLC6A4* genotype.

At the same level of significance used previously, corresponding to a maximum P value of 0.001 for cluster-generating threshold as recommended by Eklund et al. (41), there were no behavioral correlations. However, as an exploratory approach, we relaxed the stringency of the correction for multiple comparisons with a cluster-generating threshold of $P < 0.005$ as a less stringent, but still widely used, value to conduct an exploratory analysis, and a smaller extent threshold (k) of 50 voxels, which still excluded clusters too small to be of interest (details are provided in *Materials and Methods*). This analysis revealed 2 specific clusters for PC1 (Fig. 3 and Table 1): a cluster located in the right anterior insula (Fig. 3 *A–C*) and another located in the right insula proisocortex (Fig. 3 *D–F*). Both areas showed a negative relationship, with low $5-HT_{2A}$ BP corresponding to high anxiety scores (Pearson correlation: right anterior insula: $r = -0.753$, $P = 0.001$; right insula proisocortex: $r = -0.746$, $P = 0.001$; Fig. 3 *B* and *E*, respectively). Direct measurement of $5-HT_{2A}$ RNA levels within post-mortem tissue of the right anterior insula region assessed using real-time PCR mirrored this negative relationship (Pearson correlation: $r = -0.656$, $P = 0.015$; Fig. 3*C*). There was no such relationship between $5-HT_{2A}$ RNA expression and anxiety scores in the right insula proisocortex (Pearson cor-

relation: $r = -0.173$, $P = 0.571$; Fig. 3*F*). While the right anterior insula $5-HT_{2A}$ RNA expression levels correlated positively with $5-HT_{2A}$ BP (Pearson correlation: $r = 0.661$, $P = 0.014$; *SI Appendix*, Fig. S1*B*), this was not the case for the right insula proisocortex (Pearson correlation: $r = -0.466$, $P = 0.108$; *SI Appendix*, Fig. S1*C*). We used the same approach as described above to confirm the laterality of this effect, with no significant relationship between anxiety and either $5-HT_{2A}$ BP or RNA expression within these 2 regions in the left side (*SI Appendix*, Figs. S2 and S3). No significant findings were detected for PC2 at either threshold.

To determine whether these variables were also predictors of the trait anxiety scores, we performed linear regression analyses with the significant correlating variables. We included $5-HT_{2A}$ BP and RNA expression in right anterior insula and $5-HT_{2A}$ BP in right insula proisocortex as predictors and anxiety scores (PC1) as the dependent variable. All 3 variables were good predictors of anxiety scores (Table 2).

$5-HT_{2A}$ BP in the Right Anterior Insula or Insula Proisocortex Predicts the Behavioral Response to Threat after $5-HT_{2A}$ Antagonism in the HI Test. Since both PET and RNA expression provided strong evidence that $5-HT_{2A}$ in the right anterior insula and insula proisocortex contributed to overall trait anxiety scores, we next determined whether $5-HT_{2A}$ in these regions also contributed to a marmoset's responsivity to the human intruder after acute $5-HT_{2A}$ antagonism with M100907, as described above. To test this, we analyzed the relationship between $5-HT_{2A}$ BP and RNA levels and the pharmacologically induced anxiety response after $5-HT_{2A}$ antagonism. We calculated the drug-induced effect on average distance from the human threat as the percentage of change of the average distance variable following vehicle (*Materials and Methods*). This measure correlated negatively with $5-HT_{2A}$ BP in both right anterior insula (Pearson correlation: $r = -0.660$, $P = 0.014$) and insula proisocortex (Pearson correlation: $r = -0.645$, $P = 0.017$) (Fig. 4). In contrast, right anterior insula RNA expression

A Right anterior insula

D Right insula proisocortex

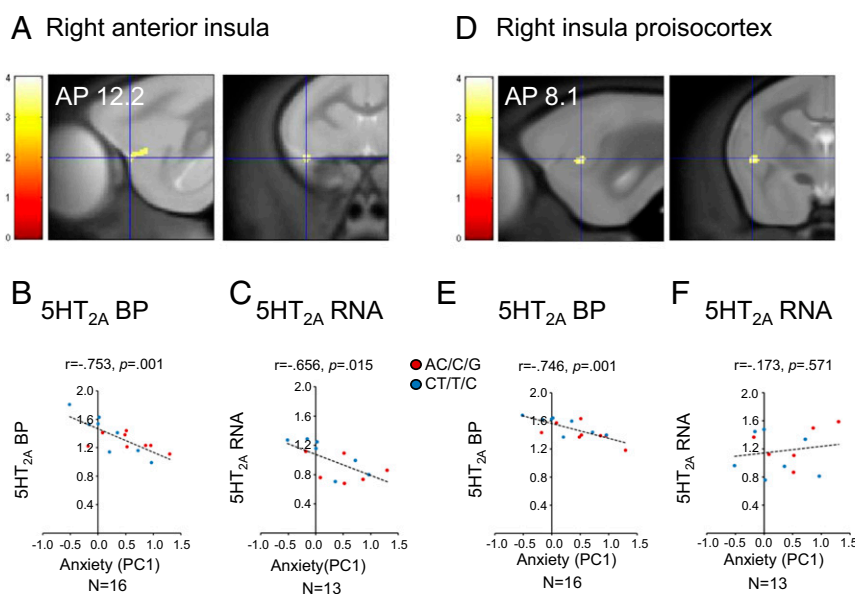**B** $5HT_{2A}$ BP **C** $5HT_{2A}$ RNA **E** $5HT_{2A}$ BP **F** $5HT_{2A}$ RNA

Fig. 3. Relation of $5HT_{2A}$ to trait anxiety scores. Voxel-based analysis correlating $5HT_{2A}$ BP with anxiety scores (PC1) derived from the population PCA of the HI test. (*A*) Specific cluster in right anterior insula (anteroposterior coordinate [AP] = 12.2) in sagittal (*Left*) and coronal (*Right*) sections centered at the highest significant peak ($t = 4.01$). Correlations between right anterior insula $5HT_{2A}$ BP (*B*; Pearson correlation: $r = -0.753$, $P = 0.001$) and $5HT_{2A}$ RNA (*C*; Pearson correlation: $r = -0.656$, $P = 0.015$) with anxiety scores (PC1) are shown. (*D*) Specific cluster in right insula proisocortex (AP = 8.1) in sagittal (*Left*) and coronal (*Right*) sections centered at the highest significant peak ($t = 3.73$). Correlation between right insula proisocortex $5HT_{2A}$ BP (*E*; Pearson correlation $r = -0.746$, $P = 0.001$) and $5HT_{2A}$ RNA (*F*; Pearson correlation $r = -0.173$, $P = 0.571$) with anxiety scores (PC1) are shown. AP coordinates from ref. 70.

Table 2. Simple linear regression, dependent variable: Human intruder anxiety scores (PC1)

	B	SE B	β
$R^2 = 0.57$, $n = 16$			
Constant	2.7	0.55	
Right anterior insula $5HT_{2A}$ BP	−1.73	0.40	−0.75**
$R^2 = 0.56$, $n = 16$			
Constant	4.28	0.93	
Right insula proisocortex $5HT_{2A}$ BP	−2.63	0.63	−0.75**
$R^2 = 0.43$, $n = 13$			
Constant	1.81	0.52	
Right anterior insula $5HT_{2A}$ RNA	−1.50	0.52	−0.66*

**$P < 0.001$; *$P < 0.05$; B, regression coefficient.

did not correlate significantly with the response to threat. A regression analysis on the significant correlating measures revealed that $5\text{-}HT_{2A}$ BP in both right anterior insula and insula proisocortex were good predictors of the increased anxiety response after $5\text{-}HT_{2A}$ antagonism (Table 3). BP of $5\text{-}HT_{2A}$ in both insula regions also highly correlated with each other (Pearson correlation: $r = 0.857$, $P = 0.0002$); thus, they were not significantly different as predictors of the threat response.

Discussion

The neurobiological mechanisms that contribute to the development of emotionally vulnerable phenotypes with increased risk for psychiatric disorders are still poorly understood. One of the most studied genetic variants within the psychiatric field is the *SLC6A4* repeat region polymorphisms, in which low-expressing variants have been associated with vulnerability to psychiatric disorders and low treatment efficacy. Here, we show that marmosets homozygous for the low-expressing, high anxiety-related *SLC6A4* variant AC/C/G show significantly reduced $5HT_{2A}$ BP and RNA expression specifically in the right posterior insula, and display an enhanced anxiety-like response to a human threat after acute systemic $5HT_{2A}$ pharmacological antagonism. In addition, we reveal that $5HT_{2A}$ BP and RNA levels in the adjacent right anterior insula and $5HT_{2A}$ BP in the right insula proisocortex have a negative relationship with trait anxiety regardless of genotype, with lower $5HT_{2A}$ levels corresponding to higher anxiety scores. Moreover, $5HT_{2A}$ BP in the right anterior insula or the right insula proisocortex were both good predictors of the size and direction of the emotional response to threat after $5HT_{2A}$ acute pharmacological antagonism.

This study not only investigates the contribution of the *SLC6A4* polymorphisms to $5HT_{2A}$ levels and its relationship with trait anxiety but also, critically, directly compares in vivo BP and post-mortem RNA expression in the same cohort of monkeys and demonstrates correspondence across measures. Our findings of reduced $5HT_{2A}$ BP and associated RNA expression in the right posterior insula of marmosets carrying the low-expressing, emotionally vulnerable *SLC6A4* variant extend previous studies, one in humans (24) and another in macaques (23), reporting reduced $5HT_{1A}$ BP in individuals homozygous for the short allele in cortical areas, including the insula. It is also consistent with a study showing reduced $5HT_{2A}$ cortical receptor binding in *SLC6A4* knockout mice (42). Besides the relationship between the *SLC6A4* variant and $5\text{-}HT_{2A}$ levels in the posterior insula, we revealed a negative relationship independent of genotype, between cortical $5HT_{2A}$ and overall anxiety scores in the adjacent right anterior insula and the more posterior insula proisocortex. While the negative relationship between BP and anxiety scores was mirrored by RNA levels in the right anterior insula, this was not the case for the insula proisocortex. Given that BP and RNA expression cor-

related positively in right anterior insula but not in insula proisocortex, a likely reason for this noncorrespondence may be due to the presence of presynaptic $5HT_{2A}$ specifically within this region. Presynaptic $5HT_{2A}$ would contribute to BP but not necessarily to RNA levels, since the RNA coding for presynaptic receptors would normally reside in cell bodies in a distal part of the brain, such as, for example, the $5HT_{2A}$-expressing thalamocortical inputs to the insula (43). Thus, depending on the overall balance between pre- and postsynaptic $5HT_{2A}$, there will be more or less correspondence between BP and RNA in different brain areas. Nonetheless, the negative relationship found between $5HT_{2A}$ BP within these 2 insula regions and anxiety scores is supported by our results from the pharmacological study in which the magnitude and direction of the behavioral response to the human intruder threat after $5HT_{2A}$ antagonism was directly associated with $5HT_{2A}$ BP within both regions (Fig. 4). A similar negative correlation between $5HT_{2A}$ and, in this case, amygdala reactivity to fearful faces has been found in medial prefrontal cortex (31), suggesting a role for prefrontal cortex $5HT_{2A}$ in the regulation of amygdala reactivity during anxiety (44). In contrast, a study in healthy volunteers using questionnaire measures of neuroticism showed a positive relationship with $5HT_{2A}$ BP in frontolimbic areas, including the left but not the right insula (45). Thus, while these studies support the role of cortical $5HT_{2A}$ in the regulation of emotion, different brain regions selectively involved in the regulation of distinct aspects of emotional behavior may show specific $5HT_{2A}$ functional patterns (46).

In the case of patients with depression, imaging and post-mortem studies show increased cortical $5HT_{2A}$ levels (30). Consistent with this, imaging studies have detected a down-regulation of $5\text{-}HT_{2A}$ receptor in the brain of such patients in response to SSRI treatment (47), and the therapeutic benefit gained by some patients when treated with a combination of both an SSRI and $5HT_{2A}$ antagonist seems to be in line with these observations (48). However, little is known about $5HT_{2A}$ levels in patients with anxiety disorders. While $5HT_{2A}$ antagonists have been used for the treatment of anxiety disorders (46), $5HT_{2A}$ agonists (serotonin hallucinogens) have provided improvement of anxiety and depressive symptoms in patients suffering from life-threatening diseases (49). Thus, the role of cortical $5HT_{2A}$ in the regulation of anxiety may depend not
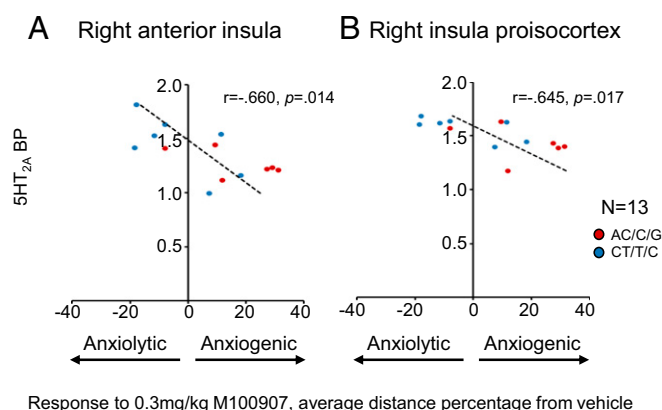

Fig. 4. Response to the human intruder threat after treatment with $5HT_{2A}$-specific antagonist M100907 (high dose [0.3 mg/kg]) in relation to $5HT_{2A}$ BP in right anterior insula (A; Pearson correlation: $r = −0.660$, $P = 0.014$) and right insula proisocortex (B; Pearson correlation: $r = −0.645$, $P = 0.017$). Response to threat was calculated as the percentage of change of average distance of the response after a 0.3-mg/kg dose relative to the response after vehicle. Values close to 0 correspond to no change from vehicle; values above and below 0 correspond to increased (enhanced anxiety) and decreased (reduced anxiety) distance, respectively.

Table 3. Simple linear regression, dependent variable: Average distance with 0.3 mg/kg of 5HT$_{2A}$ antagonist measured as the percentage of change from vehicle

	B	SE B	β
$R^2 = 0.44$, $n = 16$			
Constant	74.37	23.65	
Right anterior insula 5HT$_{2A}$ BP	−50.01	17.15	−0.66*
$R^2 = 0.42$, $n = 16$			
Constant	123.22	41.91	
Right insula proisocortex 5HT$_{2A}$ BP	−77.50	27.66	−0.64*

*$P < 0.05$; B, regression coefficient.

only on the specific brain area and type of behavior but also on the emotional context.

In the present study, the insula was the brain region that consistently showed alterations in 5-HT$_{2A}$ BP and RNA levels associated with the *SLC6A4* polymorphisms, trait anxiety scores, and anxiety-related response after 5-HT$_{2A}$ antagonism. The insula has been implicated in interoceptive processing and emotional decision making (50, 51), subjective feelings (52), emotion, and self-awareness (53). In primates, the insula cortex presents a complex structural and functional architecture, transitioning from granular neocortex in the posterior-dorsal insula to agranular neocortex in the anterior-ventral insula, with an intermediate zone of dysgranularity (54). While the posterior insula receives sensory information from the body, it is proposed that the anterior region integrates this somatic representation with cognitive information from prefrontal areas to process subjective feelings and self-awareness (17, 18). Thus, together, the posterior insula cortex and anterior insula cortex play an integrated role in emotion regulation. Consistent with this is the increased anterior insula activity during emotional processing in patients with anxiety disorders (55). In addition, in depressed patients, higher neuroticism was related to increased activity within the right anterior insula cortex to incongruent compared with congruent emotional stimuli (56). Moreover, anterior insula hyperreactivity was associated with overinterpretation of interoceptive states as threatening or negative by patients with anxiety and depression, respectively (57). Perhaps not surprisingly then, imaging studies have also shown neurophysiological changes in the insula cortex associated with *SLC6A4* polymorphism. In humans, enhanced right anterior insula activation in short allele carriers has been reported in response to an unpredictable laboratory stressor (15), fear conditioning (16), and negative self-reflection (9). Moreover, in patients with social anxiety disorder (SAD), short allele carriers showed greater anterior insula activation to fearful faces (10). In macaques, increased anterior insula activity in short allele carriers has also been shown using [^{18}F]fluoro-2-deoxy-D-glucose (FDG) PET scanning immediately after the HI test (6). The same group has also identified a positive relationship between freezing behavior in the HI test and anterior insula activity (11), which was highly heritable (58).

Here, we report a significant reduction of 5HT$_{2A}$ levels specifically in the posterior insula and an anxiogenic response to threat after 5HT$_{2A}$ antagonism, in marmosets homozygous for the high anxiety-related *SLC6A4* variant. However, it was the 5HT$_{2A}$ binding in the anterior insula, where no significant differences in 5HT$_{2A}$ levels could be detected between the *SLC6A4* genotypes, that predicted the anxiety response to threat. Thus, the *SLC6A4* polymorphism may be contributing to this differential anxiety response to threat after 5HT$_{2A}$ antagonism through altered 5HT$_{2A}$-mediated functions in posterior insula (e.g., altered processing of interoceptive information). This altered information is subsequently transferred to the anterior insula, as predicted by the model of information flow in this area

(18), where it is integrated with cognitive information from prefrontal cortex under 5HT$_{2A}$-mediated regulation, ultimately contributing to the emotional response. Although the present study clearly reveals the importance of 5HT$_{2A}$ function within the insula in relation to anxiety and the *SLC6A4* polymorphism, the extent to which this genetic association between insula activity and *SLC6A4* polymorphism is determined by 5HT$_{2A}$ density requires further investigation.

The *SLC6A4* haplotype dependency of the heightened sensitivity to acute 5HT$_{2A}$ antagonism was anticipated, since high anxious marmosets presented with reduced right insula 5HT$_{2A}$ BP and RNA levels, suggesting that further functional reduction of these receptors would have a greater behavioral impact on this haplotype. We have previously shown that these same high anxious marmosets displayed an anxiogenic response to the human intruder after an acute dose of the SSRI citalopram (35). Consistent with this, studies increasing serotonin output with acute SSRIs have shown a differential effect on right insula activation depending on the *SLC6A4* polymorphism. Smith et al. (59) found enhanced reductions in right anterior insula activity of long allele homozygotes compared with subjects homozygous for the short allele, during FDG PET after intravenous (i.v.) infusion of citalopram. In addition, oral citalopram increased amygdala and posterior insula activity in long-allele homozygotes but not short-allele ones during perception of fearful faces (60). Together, these findings demonstrate genetically driven differential insula activation in response to drugs that target the 5-HT system. Their therapeutic relevance is highlighted by recent work identifying right anterior insula metabolism as the best predictor of escitalopram treatment success (61). Based on our findings, we propose that insula 5HT$_{2A}$ levels may contribute to the mechanism by which *SLC6A4* polymorphisms modulate insula activity and subsequent anxiety responses.

In conclusion, the present study implicates 5HT$_{2A}$ receptors in the right posterior insula as the neurochemical mechanism by which genetic variation in the *SLC6A4* gene contributes to the anxious, vulnerable phenotype. We reveal a differential sensitivity to acute 5HT$_{2A}$ antagonists depending on *SLC6A4* genotype, with individuals that carry the high anxiety-related variant and present reduced right posterior insula 5HT$_{2A}$ BP and RNA levels, displaying an anxiogenic response to threat. Moreover, we show that 5HT$_{2A}$ BP in the right anterior insula and insula proisocortex were good predictors of the anxious response. Altogether, these findings highlight the specificity of the neurobiological changes associated with *SLC6A4* polymorphisms that are highly relevant to our understanding of the development and treatment of mood and anxiety disorders. Dissecting the neurobiological mechanisms underlying genetic variation that link selective brain areas and receptors to specific emotional behaviors will increase our understanding of individual differences not only in anxiety and mood disorder symptoms but also in treatment efficacy, bringing us a step closer to the development of more effective personalized therapies.

Materials and Methods

Animals and Housing. Sixteen naive common marmosets, *Callithrix jacchus*, (26 ± 2 mo, 413 ± 17 g) balanced for sex and genotype were used in this study. All animals had MRI and [^{18}F]altanserin PET scans, HI test, and snake testing [procedures described previously by Shiba et al. (62)] before entering a pharmacological study, which consisted of repeated HI test with acute intramuscular (i.m.) doses of citalopram [behavioral data reported elsewhere (35)] and, after 2 mo, with the 5HT$_{2A}$ antagonist M100907 (present study). Marmosets were bred onsite at the Innes Marmoset Colony (Behavioral and Clinical Neuroscience Institute) and housed in pairs. Temperature (24 °C) and humidity (55%) conditions were controlled, and a dawn/dusk-like 12-h period was maintained. They were provided with a balanced diet and water ad libitum. This research has been regulated under the Animals (Scientific Procedures) Act 1986 Amendment Regulations 2012 following ethical review by the University of Cambridge Animal Welfare and Ethical Review Body.

Genotyping. Marmoset were genotyped for the *SLC6A4* polymorphisms using methods previously described (35). Briefly, hair samples were taken from the animal's back. Samples were processed using a QIAamp DNA Micro Kit (Qiagen Ltd.). The primers used flanked the *SLC6A4* polymorphic repeat promoter region: RPRF (CAGACAACCGTGTTCATCTG) and RPRR (GATTC-TAGTGCCACCTAGAC). HotStarTaq Plus DNA Polymerase (Qiagen Ltd.) was used in a BioRad C1000 thermal cycler (conditions: activation for 15 min at 94 °C; 44 cycles of 30 s at 94 °C, 30 s at 55 °C, and 1 min at 72 °C; and termination after 5 min at 72 °C). The PCR product was visualized in an agarose gel, purified using a QIAquick Gel Extraction Kit (Qiagen Ltd.), and sent for sequencing (Genservice Ltd.) using the primers SeqF1 (AGCAGCACC-TAACCCTCCTA) and SeqF2 (TCCCCACTAGGCATTGCTAC).

HI Test. We have previously characterized the HI test of anxiety in marmosets using a large population (n = 52) from our colony (35). Briefly, marmosets were isolated in the upper right-hand quadrant of their home cage (separated phase). After 8 min, an unfamiliar person entered the room (intruder phase). The intruder stood in front of the cage and stared at the marmoset's eyes for 2 min. Marmoset performance was recorded with a high-definition video camera and a shotgun condenser microphone. Several measures were scored offline by an experimenter. A PCA was performed on all variables with a large cohort of marmosets, including the ones used in this study. PC1 and PC2 explained over 63% of the variance. According to variable loadings, PC1 corresponded to "anxiety" and PC2 corresponded to "coping strategy" in the emotional response to threat. The scores for each individual included in this study were derived from this population PCA and used for the subsequent imaging correlational analysis (discussed below).

PET Scan Protocol. Animals were imaged for 3 h using a microPET Focus-220 scanner (Concorde Microsystems). Anesthesia and body temperature were maintained. In addition, oxygen saturation, heart rate, and respiratory rate were measured and maintained within physiological limits throughout. Before injection, singles-mode transmission data were acquired for 515 s using a rotating ^{68}Ge point source (∼20 MBq). An attenuation correction sinogram was produced from this scan and a blank scan of the same duration using the reconstruction and segmentation software on the Focus-220 scanner. The [^{18}F]altanserin (3-[2-[4-(4-[^{18}F]fluorobenzoyl)piperidin-1-yl]ethyl]-2-sulfanylidene-1*H*-quinazolin-4-one) (0.5 ± 0.04 nmol/kg) was injected i.v. over 10 s, followed by a 5-s heparinized saline flush. For all scans, the injected amount of altanserin was ∼0.5 nmol/kg. Dynamic data were acquired in list mode for a 350- to 650-keV energy window and a 6-ns timing window. Data were subsequently histogrammed into sinograms for the following time frames: 12 × 5 s, 6 × 10 s, 3 × 20 s, 4 × 30 s, 5 × 60 s, 10 × 120 s, and 30 × 5 min. Corrections were applied for random, dead time, normalization, attenuation, and decay. Fourier rebinning (63) was used to compress the 4-dimensional sinograms to 3 dimensions before reconstruction with a 2-dimensional filtered back-projection with a Hann window cutoff at the Nyquist frequency. The image voxel size was 0.95 × 0.95 × 0.80 mm, with an array size of 128 × 128 × 95. The reconstructed images were converted to kilobecquerels per milliliter using global and slice factors determined from imaging a uniform phantom filled with a [^{18}F]fluoride solution.

PET Data Analysis. Following affine and nonlinear registration, BP maps were smoothed using an adaptive Gaussian kernel to exclude voxels outside the brain mask (the full width at half maximum was 1 mm isotropic). To assess the effect of *SLC6A4* genotype, voxel-based comparisons were made with SPM12 using a general linear model. Factors were included for genotype, sex, and weight. Two-tailed *t* tests were used to assess the main effect of genotype. A cluster-based correction for multiple comparisons was used to control the family-wise error at $P < 0.05$. The cluster-generating threshold was $P < 0.001$ (41). To investigate correlations with behavior, separate analyses were conducted with further covariates for PC1 and PC2 from the HI test. $P < 0.005$ was used as a less stringent, but still widely used, value to conduct an exploratory analysis (the most prevalent in the AFNI [Analysis of Functional NeuroImages] software, for example, from the National Institute of Mental Health, https://afni.nimh.nih.gov). An extent threshold of 50 voxels was chosen to avoid clusters too small to be of interest. We did not calculate a random-field theory threshold for this cluster size (as we did for the $P < 0.001$ threshold) to control the family-wise error directly, as Eklund et al. (41) point out that the assumptions of the calculations used do not hold for more liberal thresholds. Clusters found were followed up by RNA expression measurements within these areas.

Pharmacological Manipulation on HI Test. Due to health-related issues, only 13 of the 16 marmosets (6 AC/C/G: female [F] = 3, male [M] = 3; 7 CT/T/C: F = 4, M = 3) were available for inclusion in this next stage of the study. Animals were injected i.m. with the selective 5-HT$_{2A}$ antagonist M100907 (Sigma–Aldrich) (low dose [0.1 mg/kg] or high dose [0.3 mg/kg]) or vehicle (0.01 M phosphate-buffered saline-HCl) 25 min before the human intruder entered. M100907 doses were selected based on their reported effects on macaques (64) and squirrel monkeys (65). Repeated HI test procedures were the same as described above. To avoid habituation to the human intruder across sessions, we used different realistic rubber human masks each time (Greyland Film spol. s.r.o.). The experimental design was a Latin square randomized by sex, genotype, and masks. Treatment order was the same for all individuals (vehicle, low dose, high dose, vehicle) with 2 wk between each session. To calculate the PCA scores for each treatment, each variable was standardized using the mean and SD of the control condition (average of the 2 injections with vehicle) of the experimental subpopulation used in this study (n = 13). These standardized values were then used in the PCA function derived from the population. Average distance from the human intruder was calculated by dividing the testing quadrant into regions and scoring the time spent in each location, as previously described (35). Percentage of change from vehicle in average distance was calculated as follows: [(average distance after low or high dose of M100907/average distance after vehicle) × 100] − 100. Planned comparisons were performed using paired 2-tailed *t* tests.

Real-Time PCR. At the end of the study, animals were premedicated with ketamine hydrochloride before being euthanized with pentobarbital sodium (Dolethal; 1 mL of a 200-mg/mL solution; Merial Animal Health). Brain were dissected, frozen using liquid nitrogen, and kept at −80 °C until use. The brains were then sliced in a cryostat at −20 °C to 200-μm-thick sections. Tissue samples for each target region were excised using punches of 1.5- and 2-mm radio length (*SI Appendix*, Fig. S5). Total RNA was extracted with the RNeasy Plus Universal Mini Kit (Qiagen Ltd.) in accordance with the manufacturer's protocol. Samples were quantified using a NanoDrop spectrometer (Thermo Fisher Scientific) with an average concentration of 9.40 ± 0.24 ng/μL. RNA integrity, analyzed using an Agilent RNA 6000 Pico Kit with an Agilent 2100 Bioanalyzer instrument, had an average RNA integrity number (RIN) of 8.60 ± 0.04. Samples were stored at −80 °C until use. Complementary DNA (cDNA) synthesis and real-time qPCR were performed using a Brilliant II SYBR Green QRT-PCR Master Mix Kit, 1-Step (Agilent Technologies), adding 2 μL of sample into each primer combination reaction. Primers for the 5HT$_{2A}$ gene were designed using Primer-BLAST, a software tool from the National Center for Biotechnology Information (66). The predicted 5HT$_{2A}$ messenger RNA sequence used to design the primers was obtained from the Ensembl database (67). Four marmoset-specific reference genes were selected: ACTB (β-actin), TBP (TATA-box binding protein), GAPDH (glyceraldehyde-3-phosphate dehydrogenase) (68), and SDHA (succinate dehydrogenase complex, subunit A) (68, 69). All primer combinations were designed to span exon-exon boundaries (primer sequences are shown in *SI Appendix*, Table S3). All reactions were performed in duplicate for each individual and control (conditions: cDNA synthesis for 30 min at 50 °C, activation step for 10 min at 95 °C, 40 2-step cycle of denaturation 30 s at 95 °C, and combined annealing/extension for 1 min at 60 °C, with final melting curves to check the specificity of the product) using the Bio-Rad CFX96 Touch Real-Time PCR Detection System. Results were obtained using BioRad CFXManager software. Using specific amplification efficiencies for each primer set previously calculated and an interrun calibrator, we ran a gene study where the relative expression levels of the gene of interest (5HT$_{2A}$) were normalized to the 4 reference genes (ACTB, TBP, GAPDH, and SDHA) and calculated using the ΔΔCq mathematical method: $R = [(E_{target})^{DCq_{target}(\text{Mean control} - \text{Mean sample})}]/[(E_{Ref\ index})^{DCq_{Ref\ index}(\text{Mean control} - \text{Mean sample})}]$, where the ratio (R) is calculated based on the amplification efficiencies (E) of the gene of interest (target) and multiple references genes (Ref index) using the difference between the quantification cycle (Cq) for each sample and control.

Statistical Analysis. Analyses were performed using SPSS Statistics (version 24; IBM Corp.). Data are presented as mean ± SEM, and $P ≤ 0.05$ was considered statistically significant. After confirming normal distribution and homogeneity of variance, one-way ANOVA and Pearson correlations were performed.

1. T. Canli, K.-P. Lesch, Long story short: The serotonin transporter in emotion regulation and social cognition. *Nat. Neurosci.* **10**, 1103–1109 (2007).
2. K. P. Lesch *et al.*, Association of anxiety-related traits with a polymorphism in the serotonin transporter gene regulatory region. *Science* **274**, 1527–1531 (1996).
3. A. J. Bennett *et al.*, Early experience and serotonin transporter gene variation interact to influence primate CNS function. *Mol. Psychiatry* **7**, 118–122 (2002).
4. A. R. Hariri *et al.*, Serotonin transporter genetic variation and the response of the human amygdala. *Science* **297**, 400–403 (2002).
5. T. Canli *et al.*, Neural correlates of epigenesis. *Proc. Natl. Acad. Sci. U.S.A.* **103**, 16033–16038 (2006).
6. N. H. Kalin *et al.*, The serotonin transporter genotype is associated with intermediate brain phenotypes that depend on the context of eliciting stressor. *Mol. Psychiatry* **13**, 1021–1027 (2008).
7. F. Klumpers *et al.*, Dorsomedial prefrontal cortex mediates the impact of serotonin transporter linked polymorphic region genotype on anticipatory threat reactions. *Biol. Psychiatry* **78**, 582–589 (2015).
8. T. Klucken *et al.*, The association between the 5-HTTLPR and neural correlates of fear conditioning and connectivity. *Soc. Cogn. Affect. Neurosci.* **10**, 700–707 (2015).
9. Y. Ma *et al.*, 5-HTTLPR polymorphism modulates neural mechanisms of negative self-reflection. *Cereb. Cortex* **24**, 2421–2429 (2014).
10. H. Klumpp *et al.*, Serotonin transporter gene alters insula activity to threat in social anxiety disorder. *Neuroreport* **25**, 926–931 (2014).
11. A. J. Shackman *et al.*, Neural mechanisms underlying heterogeneity in the presentation of anxious temperament. *Proc. Natl. Acad. Sci. U.S.A.* **110**, 6145–6150 (2013).
12. L. Pezawas *et al.*, 5-HTTLPR polymorphism impacts human cingulate-amygdala interactions: A genetic susceptibility mechanism for depression. *Nat. Neurosci.* **8**, 828–834 (2005).
13. J. Pacheco *et al.*, Frontal-limbic white matter pathway associations with the serotonin transporter gene promoter region (5-HTTLPR) polymorphism. *J. Neurosci.* **29**, 6229–6233 (2009).
14. M. K. Madsen *et al.*, Threat-related amygdala functional connectivity is associated with 5-HTTLPR genotype and neuroticism. *Soc. Cogn. Affect. Neurosci.* **11**, 140–149 (2016).
15. E. M. Drabant *et al.*, Neural mechanisms underlying 5-HTTLPR-related sensitivity to acute stress. *Am. J. Psychiatry* **169**, 397–405 (2012).
16. A. Hermann *et al.*, Functional gene polymorphisms in the serotonin system and traumatic life events modulate the neural basis of fear acquisition and extinction. *PLoS One* **7**, e44352 (2012).
17. T. Singer *et al.*, Empathy for pain involves the affective but not sensory components of pain. *Science* **303**, 1157–1162 (2004).
18. A. D. Craig, The sentient self. *Brain Struct. Funct.* **214**, 563–577 (2010).
19. H. P. Jedema *et al.*, Cognitive impact of genetic variation of the serotonin transporter in primates is associated with differences in brain morphology rather than serotonin neurotransmission. *Mol. Psychiatry* **15**, 512–522, 446 (2010).
20. B. T. Christian *et al.*, Serotonin transporter binding and genotype in the nonhuman primate brain using [C-11]DASB PET. *Neuroimage* **47**, 1230–1236 (2009).
21. R. V. Parsey *et al.*, Effect of a triallelic functional polymorphism of the serotonin-transporter-linked promoter region on expression of serotonin transporter in the human brain. *Am. J. Psychiatry* **163**, 48–51 (2006).
22. N. V. Murthy *et al.*, Serotonin transporter polymorphisms (SLC6A4 insertion/deletion and rs25531) do not affect the availability of 5-HTT to [11C] DASB binding in the living human brain. *Neuroimage* **52**, 50–54 (2010).
23. B. T. Christian *et al.*, Serotonin transporter genotype affects serotonin 5-HT1A binding in primates. *J. Neurosci.* **33**, 2512–2516 (2013).
24. S. P. David *et al.*, A functional genetic variation of the serotonin (5-HT) transporter affects 5-HT1A receptor binding in humans. *J. Neurosci.* **25**, 2586–2590 (2005).
25. R. Keers *et al.*, Interaction between serotonin transporter gene variants and life events predicts response to antidepressants in the GENDEP project. *Pharmacogenomics J.* **11**, 138–145 (2011).
26. E. Penn, D. K. Tracy, The drugs don't work? Antidepressants and the current and future pharmacological management of depression. *Ther. Adv. Psychopharmacol.* **2**, 179–188 (2012).
27. C. J. Harmer, P. J. Cowen, 'It's the way that you look at it'–A cognitive neuropsychological account of SSRI action in depression. *Philos. Trans. R. Soc. Lond. B Biol. Sci.* **368**, 20120407 (2013).
28. G. Quesseveur, H. T. Nguyen, A. M. Gardier, B. P. Guiard, 5-HT2 ligands in the treatment of anxiety and depression. *Expert Opin. Investig. Drugs* **21**, 1701–1725 (2012).
29. D. Arnone, J. Horder, P. J. Cowen, C. J. Harmer, Early effects of mirtazapine on emotional processing. *Psychopharmacology (Berl.)* **203**, 685–691 (2009).
30. J. B. Savitz, W. C. Drevets, Neuroreceptor imaging in depression. *Neurobiol. Dis.* **52**, 49–65 (2013).
31. P. M. Fisher *et al.*, Medial prefrontal cortex 5-HT(2A) density is correlated with amygdala reactivity, response habituation, and functional coupling. *Cereb. Cortex* **19**, 2499–2507 (2009).
32. P. M. Fisher *et al.*, Medial prefrontal cortex serotonin 1A and 2A receptor binding interacts to predict threat-related amygdala reactivity. *Biol. Mood Anxiety Disord.* **1**, 2 (2011).
33. L. H. Pinborg *et al.*, The 5-HT2A receptor binding pattern in the human brain is strongly genetically determined. *Neuroimage* **40**, 1175–1180 (2008).
34. E. Pascale *et al.*, Monomorphic region of the serotonin transporter promoter gene in New World monkeys. *Am. J. Primatol.* **74**, 1028–1034 (2012).
35. A. M. Santangelo *et al.*, Novel primate model of serotonin transporter genetic polymorphisms associated with gene expression, anxiety and sensitivity to antidepressants. *Neuropsychopharmacology* **41**, 2366–2376 (2016).
36. L. Oikonomidis *et al.*, A dimensional approach to modeling symptoms of neuropsychiatric disorders in the marmoset monkey. *Dev. Neurobiol.* **77**, 328–353 (2017).
37. C. T. Miller *et al.*, Marmosets: A neuroscientific model of human social behavior. *Neuron* **90**, 219–233 (2016).
38. J. C. Izpisua Belmonte *et al.*, Brains, genes, and primates. *Neuron* **86**, 617–631 (2015).
39. P. J. Riss *et al.*, Validation and quantification of [18F]altanserin binding in the rat brain using blood input and reference tissue modeling. *J. Cereb. Blood Flow Metab.* **31**, 2334–2342 (2011).
40. G. J. Carey, B. Costall, A. M. Domeney, D. N. Jones, R. J. Naylor, Behavioural effects of anxiogenic agents in the common marmoset. *Pharmacol. Biochem. Behav.* **42**, 143–153 (1992).
41. A. Eklund, T. E. Nichols, H. Knutsson, Cluster failure: Why fMRI inferences for spatial extent have inflated false-positive rates. *Proc. Natl. Acad. Sci. U.S.A.* **113**, 7900–7905 (2016).
42. A. Rioux *et al.*, Adaptive changes of serotonin 5-HT2A receptors in mice lacking the serotonin transporter. *Neurosci. Lett.* **262**, 113–116 (1999).
43. A. Barre *et al.*, Presynaptic serotonin 2A receptors modulate thalamocortical plasticity and associative learning. *Proc. Natl. Acad. Sci. U.S.A.* **113**, E1382–E1391 (2016).
44. S. Aznar, A. B. Klein, Regulating prefrontal cortex activation: An emerging role for the 5-HT$_2$A serotonin receptor in the modulation of emotion-based actions? *Mol. Neurobiol.* **48**, 841–853 (2013).
45. V. G. Frokjaer *et al.*, Frontolimbic serotonin 2A receptor binding in healthy subjects is associated with personality risk factors for affective disorder. *Biol. Psychiatry* **63**, 569–576 (2008).
46. L. Moulédous, P. Roullet, B. P. Guiard, "Brain circuits regulated by the 5-HT2A receptor: Behavioural consequences on anxiety and fear memory" in *5-HT2A Receptors in the Central Nervous System* (Springer International Publishing, Cham, 2018), pp. 231–258.
47. J. H. Meyer *et al.*, The effect of paroxetine on 5-HT(2A) receptors in depression: An [(18)F]setoperone PET imaging study. *Am. J. Psychiatry* **158**, 78–85 (2001).
48. G. J. Marek, L. L. Carpenter, C. J. McDougle, L. H. Price, Synergistic action of 5-HT2A antagonists and selective serotonin reuptake inhibitors in neuropsychiatric disorders. *Neuropsychopharmacology* **28**, 402–412 (2003).
49. S. Reiche *et al.*, Serotonergic hallucinogens in the treatment of anxiety and depression in patients suffering from a life-threatening disease: A systematic review. *Prog. Neuropsychopharmacol. Biol. Psychiatry* **81**, 1–10 (2018).
50. A. D. Craig, How do you feel? Interoception: The sense of the physiological condition of the body. *Nat. Rev. Neurosci.* **3**, 655–666 (2002).
51. B. D. Dunn *et al.*, Can you feel the beat? Interoceptive awareness is an interactive function of anxiety- and depression-specific symptom dimensions. *Behav. Res. Ther.* **48**, 1133–1138 (2010).
52. H. D. Critchley, S. Wiens, P. Rotshtein, A. Öhman, R. J. Dolan, Neural systems supporting interoceptive awareness. *Nat. Neurosci.* **7**, 189–195 (2004).
53. A. D. Craig, How do you feel–now? The anterior insula and human awareness. *Nat. Rev. Neurosci.* **10**, 59–70 (2009).
54. A. L. Bauernfeind *et al.*, A volumetric comparison of the insular cortex and its subregions in primates. *J. Hum. Evol.* **64**, 263–279 (2013).
55. H. Klumpp, D. Post, M. Angstadt, D. A. Fitzgerald, K. L. Phan, Anterior cingulate cortex and insula response during indirect and direct processing of emotional faces in generalized social anxiety disorder. *Biol. Mood Anxiety Disord.* **3**, 7 (2013).
56. J. C. Fournier *et al.*, Neuroticism and individual differences in neural function in unmedicated major depression: Findings from the EMBARC study. *Biol. Psychiatry Cogn. Neurosci. Neuroimaging* **2**, 138–148 (2017).
57. M. P. Paulus, M. B. Stein, Interoception in anxiety and depression. *Brain Struct. Funct.* **214**, 451–463 (2010).
58. A. S. Fox *et al.*, Intergenerational neural mediators of early-life anxious temperament. *Proc. Natl. Acad. Sci. U.S.A.* **112**, 9118–9122 (2015).
59. G. S. Smith *et al.*, Effects of serotonin transporter promoter polymorphisms on serotonin function. *Neuropsychopharmacology* **29**, 2226–2234 (2004).
60. Y. Ma *et al.*, Allelic variation in 5-HTTLPR and the effects of citalopram on the emotional neural network. *Br. J. Psychiatry* **206**, 385–392 (2015).
61. C. L. McGrath *et al.*, Toward a neuroimaging treatment selection biomarker for major depressive disorder. *JAMA Psychiatry* **70**, 821–829 (2013).
62. Y. Shiba *et al.*, Individual differences in behavioral and cardiovascular reactivity to emotive stimuli and their relationship to cognitive flexibility in a primate model of trait anxiety. *Front. Behav. Neurosci.* **8**, 137 (2014).
63. M. Defrise *et al.*, Exact and approximate rebinning algorithms for 3-D PET data. *IEEE Trans. Med. Imaging* **16**, 145–158 (1997).
64. K. S. Murnane, M. L. Andersen, K. C. Rice, L. L. Howell, Selective serotonin 2A receptor antagonism attenuates the effects of amphetamine on arousal and dopamine overflow in non-human primates. *J. Sleep Res.* **22**, 581–588 (2013).
65. W. E. Fantegrossi *et al.*, Role of dopamine transporters in the behavioral effects of 3,4-methylenedioxymethamphetamine (MDMA) in nonhuman primates. *Psychopharmacology (Berl.)* **205**, 337–347 (2009).
66. J. Ye *et al.*, Primer-BLAST: A tool to design target-specific primers for polymerase chain reaction. *BMC Bioinformatics* **13**, 134 (2012).
67. P. Flicek *et al.*, Ensembl 2014. *Nucleic Acids Res.* **42**, D749–D755 (2014).
68. Y. Shimamoto *et al.*, Selection of suitable reference genes for mRNA quantification studies using common marmoset tissues. *Mol. Biol. Rep.* **40**, 6747–6755 (2013).
69. Y. Fujii *et al.*, Immune-related gene expression profile in laboratory common marmosets assessed by an accurate quantitative real-time PCR using selected reference genes. *PLoS One* **8**, e56296 (2013).
70. Paxinos G, Watson C, Petrides M, Rosa M, Tokuno H, *The Marmoset Brain in Stereotaxic Coordinates* (Academic Press, Ed. 1, 2012).